LEGIBILITY NOTICE

A major purpose of the Technical Information Center is to provide the broadest dissemination possible of information contained in DOE's Research and Development Reports to business, industry, the academic community, and federal, state and local governments.

Although portions of this report are not reproducible, it is being made available in microfiche to facilitate the availability of those parts of the document which are legible.

3

LA-UR -87-779

26

LA-UR--87-779

DE87 007478

Los Alamos National Laboratory is operated by the University of California for the United States Department of Energy under contract W-7405-ENG-36

TITLE TRANSIENT ANALYSIS OF A COUPLED ACCELERATOR AND DECELERATOR SYSTEM

AUTHOR(S) H. Takeda

SUBMITTED TO 1987 Particle Accelerator Conference, Washington, DC, March 16-19, 1987

DISCLAIMER

This report was prepared as an account of work sponsored by an agency of the United States Government. Neither the United States Government nor any agency thereof, nor any of their employees, makes any warranty, express or implied, or assumes any legal liability or responsibility for the accuracy, completeness, or usefulness of any information, apparatus, product, or process disclosed, or represents that its use would not infringe privately owned rights. Reference herein to any specific commercial product, process, or service by trade name, trademark, manufacturer, or otherwise does not necessarily constitute or imply its endorsement, recommendation, or favoring by the United States Government or any agency thereof. The views and opinions of authors expressed herein do not necessarily state or reflect those of the United States Government or any agency thereof.

By acceptance of this article, the publisher recognizes that the U.S. Government retains a nonexclusive, royalty-free license to publish or reproduce the published form of this contribution, or to allow others to do so, for U.S. Government purposes.

The Los Alamos National Laboratory requests that the publisher identify this article as work performed under the auspices of the U.S. Department of Energy

Los Alamos National Laboratory
Los Alamos, New Mexico 87545

FORM NO 836 R4
ST NO 2629 5/81

DISTRIBUTION OF THIS DOCUMENT IS UNLIMITED

TRANSIENT ANALYSIS OF A COUPLED ACCELERATOR AND DECELERATOR SYSTEM*

Harunori Takeda, MS-H820
Los Alamos National Laboratory, Los Alamos, NM 87545

Abstract

For an energy-efficient accelerator system to be used for a free-electron laser, the stability of an energy recovery system utilizing a bridge coupler placed between the accelerator and the decelerator is studied numerically. Energy is recovered by recirculating the accelerated electron beam through the decelerator; the recovered energy is then transported through the bridge coupler to the accelerator. The calculation shows that a large transient voltage oscillation is induced in the system. This transient oscillation can be reduced significantly by slowly applying both the electron-beam current and the klystron power at the beginning. Two types of instabilities are predicted according to the scraping of the electron beam between the accelerator and the decelerator. When the energy spectrum of the electron beam is scraped at the high end, the system induces an oscillation. However, when the low-energy end is scraped, the electron recirculation may stop unless the klystron power is boosted by a feedback system.

Introduction

To increase the energy efficiency in the free electron laser system, a decelerator is added to collect the energy of the electron beam and to recirculate it to an accelerator. The system consists of bridge-coupler cavities, accelerator cavities, an undulator, and decelerator cavities. The bridge coupler feeds energy from the klystron into the accelerator and couples the energy flow from the decelerator to the accelerator. The accelerator is followed by a drift space and an undulator. The electron beam interacts with the undulator field and laser, transferring energy to the laser. To simplify the argument, we ignore the energy loss of the electron beam in the undulator. After the electron beam passes a 180° bend, it is guided to the decelerator. The decelerator takes the energy from the electron beam and recirculates it to the accelerator through the bridge coupler.

We simulate the system numerically to explore the stability of the rf voltage in each cavity and to explore the stability of both the electron beam current and the energy. We also evaluate the system stability when the currents are scraped: the beam transport system loses current, and the scraper between the accelerator and the undulator reduces the recirculated currents. As the electrons are accelerated, the energy spectrum of the electrons changes its peak energy while maintaining the same spectral shape. The amount of beam scraping is determined by the fraction of the spectrum cut out while passing through a fixed energy window. The detailed analytic description of this work is presented in a companion paper.[1]

System Representation with Parallel Resonant Circuits

The simulated system consists of elements for an accelerator, a decelerator, and a bridge coupler. For the electron beam that passes through the system, the electron beam energy and current are time dependent. The electron beam energy at the accelerator depends on the phase and amplitude of the rf, and the electron beam current at the decelerator depends on the amount of current scraping, which, in turn, depends on the electron beam energy at the accelerator.

With an analogy to electrical circuits, we formulate the system with coupled resistance inductance capacitance (RLC) circuits. In our system, the average current of the electron beam and the equivalent klystron current drive the voltage for each element. Using the analogy of parallel RLC circuits, we can set up circuit equations for the beam currents and for the induced voltages. The accelerator cavities, consisting of tanks of 11 cells and 15 cells, are treated as one resonant RLC element. Also, the decelerator is represented with one RLC element. The bridge coupler has cavities, and it is represented by three coupled RLC elements because the voltages in the connecting cavities can help clarify the excited modes.

*Work performed under the auspices of the U.S. Department of Energy and supported by the U.S. Army Strategic Defense Command.

The Equations Describing the Accelerator, the Decelerator, and the Bridge Coupler

The system is described by five inductively coupled RLC circuits. The coupling constants k_{ij} are related to mutual inductance M_{ij} between the ith and jth element given as $k_{ij} = M_{ij}/\sqrt{L_i L_j}$. The shunt resistance R_j, cavity Q_j, and the cavity capacitance C_j form an RLC circuit for a jth element. The relations between them for an isolated parallel circuit are

$$R_j C_j = \frac{Q_j}{\omega_j}$$

and

$$L_j C_j = \frac{1}{\omega_j^2} . \qquad (1)$$

The characteristic frequency ω_j for the jth element must also satisfy the following condition: At the klystron frequency ω_0, which is equal to 1300 MHz, all the elements of the coupled circuits must resonate when the intraelement coupling reduces to zero. This condition is formulated as the diagonal elements of the eigenmatrix for a stationary system equal to unity:

$$\begin{aligned} 2y_1 f_1^2 &= 1 \\ (y_1 + y_2) f_2^2 &= 1 \\ (y_2 + y_3) f_3^2 &= 1 \\ (y_3 + y_4) f_4^2 &= 1 \\ 2y_4 f_5^2 &= 1 , \end{aligned} \qquad (2)$$

The stationary system assumes no driving terms and assumes nondissipative cavities. In Eq. (2), y_i is defined as $1/(1 - k_i^2)$, and f_j is defined as ω_j/ω_0. By solving Eq. (2), the characteristic frequencies ω_j are expressed as functions of coupling constants k_{ij}.

The driving terms of the coupled circuits are the klystron-frequency component of the electron-beam current at the accelerator, the current equivalent of klystron power, and the klystron-frequency component of the electron beam current at the decelerator. Because there is a time delay between the exit of the accelerator and the entrance of the decelerator, the electron-beam phase varies at the entrance of the decelerator. The phase variation, with respect to the reference klystron, depends on the electron-beam energy at the exit of the accelerator. The phase slippage of electrons in the accelerator or in the decelerator is neglected.

The oscillating rf voltages in each element can be represented as a superposition of five dominant modes. These modes are obtained by solving eigenequations in a stationary configuration: setting the Q of the cavities equal to ∞ and ignoring the driving terms. The voltage profile at each element for each stationary mode is shown in Fig. 1. The mode with the highest frequency is shown at the top with the dotted 0 V

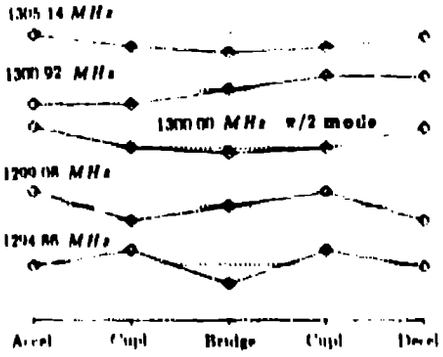

Fig. 1. Voltage mode patterns at each element.

MASTER

DISTRIBUTION OF THIS DOCUMENT IS UNLIMITED

reference line; the mode with lowest frequency is shown at the bottom. The third line from the top is the $\pi/2$ mode with which the accelerator or decelerators are designed to operate at the 1301-MHz frequency. This mode has nodes at the coupling cells in the bridge coupler. Using the parameters described later, the frequency of each mode calculated from the eigenvalue analysis are 1294.86 MHz, 1299.05 MHz, 1301.[illegible] MHz, [illegible] MHz and 1307.14 MHz.

The Equations Describing a Transient State

The return electron beam acts as a time-delayed feedback to the system. The system behavior for such a configuration is not well known. To answer the questions of when the stationary state is established, how stable it depends on the energy scraping window, or how sensitive it depends on electron beam current, we obtain the equations for the transient state of the system, which begins when the electron beam enters the excited accelerator cavities.

By subtracting the equations for the stationary system from the equations that describe the general system, the equations for transient state can be obtained. Defining u_i as the complex transient voltage $U_i e^{j\omega t}$ multiplied by $\sqrt{C_{ij}}$, the transient state equations are

$$\frac{1}{\omega}\left[P_1\left(\frac{\omega_1}{\omega}\right)+2j\right]\dot{u}_1+\left[2y_1\left(\frac{\omega_1}{\omega}\right)^2-1+jP_1\right]u_1+\sqrt{2}k_1y_1\left(\frac{\omega_1}{\omega}\right)\left(\frac{\omega_2}{\omega}\right)u_2=j\frac{1}{\sqrt{C_{1\omega}}}(I_{1R}-I_{10}e^{j\Psi_1})$$

$$\sqrt{2}k_1y_1\left(\frac{\omega_1}{\omega}\right)\left(\frac{\omega_2}{\omega}\right)\dot{u}_1+\frac{1}{\omega}\left[P_2\left(\frac{\omega_2}{\omega}\right)+2j\right]\dot{u}_2+\left[(y_2+y_{21})\left(\frac{\omega_2}{\omega}\right)^2-1+jP_2\right]u_2+k_2y_2\left(\frac{\omega_2}{\omega}\right)\left(\frac{\omega_1}{\omega}\right)\dot{u}_1=0$$

$$k_2y_2\left(\frac{\omega_2}{\omega}\right)\left(\frac{\omega_1}{\omega}\right)\dot{u}_2+\frac{1}{\omega}\left[P_3\left(\frac{\omega_3}{\omega}\right)+2j\right]\dot{u}_3+\left[(y_3+y_{31})\left(\frac{\omega_3}{\omega}\right)^2-1+jP_3\right]u_3+k_3y_3\left(\frac{\omega_3}{\omega}\right)\left(\frac{\omega_1}{\omega}\right)\dot{u}_1=j\frac{1}{\sqrt{C_{3\omega}}}(\Delta I\tan\Psi_3)$$

$$k_3y_3\left(\frac{\omega_3}{\omega}\right)\left(\frac{\omega_1}{\omega}\right)\dot{u}_3+\frac{1}{\omega}\left[P_4\left(\frac{\omega_4}{\omega}\right)+2j\right]\dot{u}_4+\left[(y_4+y_{41})\left(\frac{\omega_4}{\omega}\right)^2-1+jP_4\right]u_4+\sqrt{2}k_4y_4\left(\frac{\omega_4}{\omega}\right)\left(\frac{\omega_5}{\omega}\right)\dot{u}_5=0$$

$$\sqrt{2}k_4y_4\left(\frac{\omega_4}{\omega}\right)\left(\frac{\omega_5}{\omega}\right)\dot{u}_4+\frac{1}{\omega}\left[P_5\left(\frac{\omega_5}{\omega}\right)+2j\right]u_5+\left[2y_5\left(\frac{\omega_5}{\omega}\right)^2-1+jP_5\right]u_5=\frac{j}{\sqrt{C_{5\omega}}}(I_5e^{j\Psi_5}-I_{5m}e^{j\Psi_{5m}})+\frac{j\Psi_5}{\sqrt{C_{5\omega}}}I_5e^{j\Psi_5} \qquad (3)$$

where P is defined as $1/Q$, $(I_{1R}-I_{10}e^{j\Psi_1})$ is the ramped electron beam current that enters the accelerator with amplitude I_{10}, and $\Delta I\tan\Psi_3$ is the equivalent current of the klystron power entering the bridge coupler. The klystron power ramping is included in ΔI. The transient voltage and phase at the decelerator are driven by a difference between return electron current and the reference stationary current. The reference phase Ψ_{5m} and amplitude I_{5m} of the stationary current assumes no scraping. Also, the transient voltage and phase at the decelerator are driven by a derivative of the arrival phase of the return electrons. To include the time delay of the return electron beam, this decelerator driving term is evaluated at a time when the electron beam leaves the accelerator.

In general, the transient state defined as a vector of complex voltages of each element can be expressed as a superposition of the five stationary eigenvectors. Because the system resonates at the $\pi/2$ mode before the electron beam loading, the mixture of the other four modes occurring in the transient state can be interpreted as a result of the interaction between the electron beam and the cavity system.

Beam Loading and Initial Transient RF Voltages.

Before the electron beam loads into the accelerator, only the klystron power drives the system. The system is in a stationary state. When an electron beam gains energy in the accelerator cavity, the stationary state is modified because of the beam loading. The difference between the stationary states, one beam loaded and the other not beam loaded, is the initial transient voltage. If the magnitude of the transient voltage is larger than the energy acceptance window of the scraper, a part of the electron beam is scraped and fewer electrons enter the decelerator. The recovered energy at the decelerator decreases, and the energy recirculated to the accelerator decreases. If the scraping occurred at the low energy end of the electron beam, the accelerated energy of the following electron beam is more out of the energy acceptance window and fewer electrons pass the window. The stored energy in the system is reduced, and none of the electrons arriving later at the accelerator pass the acceptance window when the scraping occurs at the low energy end of the beam.

When the high energy end of the beam is scraped, the electron pulses arriving later at the accelerator are less accelerated. More electrons may pass the energy acceptance window, and the system regains the energy by decelerating more electrons. As a result, the transient state can oscillate without reaching a stationary state.

The energy distribution of the electron beam as shown in Fig. 2 is used to calculate the part of current scraped in the

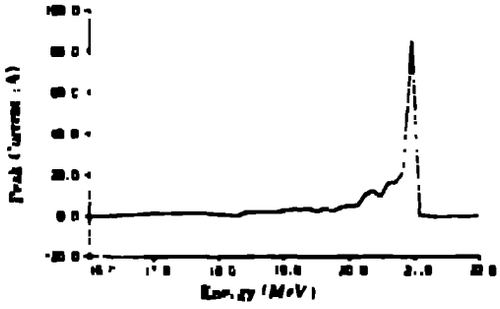

Fig. 2 The electron energy distribution

numerical simulation. The energy of the peak of distribution is set equal to the energy of the accelerated electron beam.

Accelerator and Electron-Beam Parameters[2]

We assume 15 equivalent cells for the accelerator or for the decelerator to simplify the numerical calculation. Designating (A) for accelerator structure, (D) for decelerator structure, and (B) for bridge coupler, the parameters for the equivalent parallel circuit are

Shunt impedence	R_A	R_D = 86 (MΩ),
	R_B	= 5.76 (MΩ),
Quality Factor	Q_A	Q_D = 18×10^3,
	Q_B	= 2×10^3,
Length of Cavity	l_A	l_D = 11.527 (cm) × 15 = 172.91 (cm),
	l_B	= 11.527 (cm),
Coupling Constants	k_1	= 2×10^{-3}, k_2 = 1.1×10^{-2},
	k_3	= 1.1×10^{-2}, k_4 = 1×10^{-3}
Capacitance	C_A	C_D = $\frac{S_A}{\omega_0}$ = 2.55×10^{-10} (F),
and Inductance	L_A	L_D = $\frac{1}{\omega_0 S_A}$ = 5.878×10^{-10} (H)
	C_B	= $\frac{S_B}{\omega_0}$ = 4.25×10^{-10} (F),
	L_B	= $\frac{1}{\omega_0 S_B}$ = 3.527×10^{-10} (H)

where $\frac{S_A}{\omega_0}$ = 1.36 (H).

The electron beam current component for the $\pi/2$ frequency is approximately equal to the electron beam current averaged over a macropulse. We assume the average beam current of 115.6 mA or 16.2 mA.

An Instability of Scraping Beam at Low Energy and an Instability of Scraping at High Energy

We gradually ramp the average electron beam current to the maximum 115 mA during the first 1 μs. The slow ramping of the electron beam reduces the transient oscillation of the voltage. The electron beam window is assumed to be [illegible] (A)

This is an 8% energy window. As seen in Fig. 3, the electron beam scraped as much as 23% at 4 μs immediately loses its current when the low-energy end of the b[illegible] starts scraping at 12 μs; no electron current is arriving at the decelerator at 15 μs. The beam-loaded voltage at the accelerator is shown in Fig. 4. For the first 15 μs, it droops a few megavolts and droops down to about 17 MV after 25 μs. However, with the beam current at 46.2 mA, the drooping is much slower and the beam still recirculates at 30 μs.

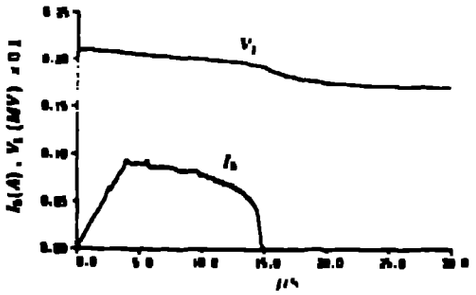

Fig. 3 Drooping of recirculated current.

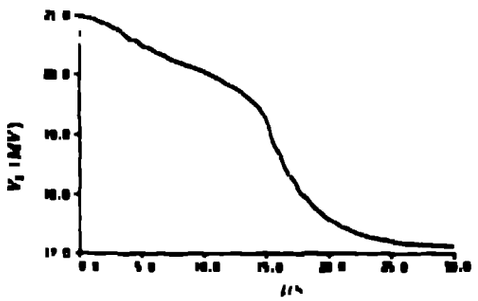

Fig. 4 Drooping of accelerator voltage.

To compensate for the energy drooping of the system because of the beam scraping, we jump the klystron power linearly by 1% at the first 1 μs. The system becomes stable, and the initial transient oscillation damps, as shown in Fig. 5, for the accelerator voltage amplitude. However, the system stability is violated easily with a small change of klystron power. A threshold where the instability starts (recirculated electron current dies) is searched by raising the low end of the energy window. The threshold, in terms of a ratio of electron beam current scraped to the total beam current, was about 25%. However, for a setup with a total beam current of 46.2 mA, the threshold is higher; it is about 50%.

Lowering the energy window so that the high end of the energy distribution is scraped, the system exhibits a periodic oscillation; the recirculated electron beam current is partially scraped and restores periodically (Fig. 6). The voltage amplitudes at the accelerator and decelerator are shown in Figs. 7 and 8, respectively. At the peak of the accelerating voltage, the current is at its minimum. At the minimum of the accelerating voltage, the current is at the maximum. The phase difference

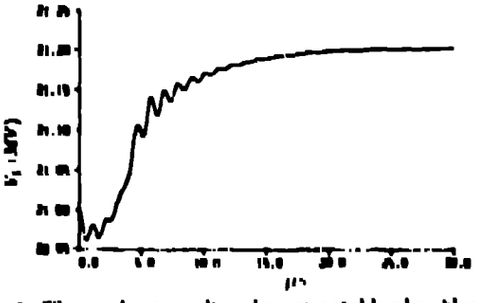

Fig. 5 The accelerator voltage becomes stable when klystron power is boosted

between the decelerator voltage, as shown in Fig. 8, and the accelerator voltage is π; this shows that the second or fourth mode in Fig. 1 is excited. The oscillation frequency of the accelerator voltage is about 0.9 MHz, as obtained from Fig. 7. This is consistent with the frequency of the second or fourth mode obtained from the eigenanalysis.

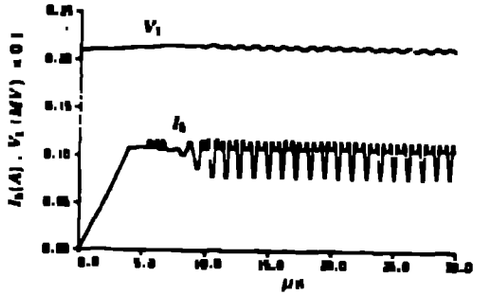

Fig. 6 The beam scraping at the high-energy end induces oscillation in recirculated current.

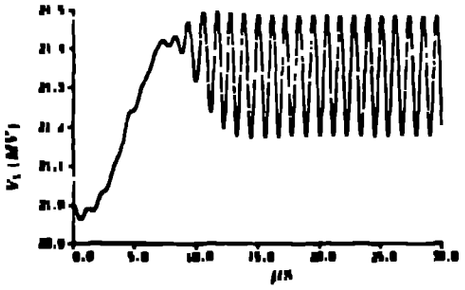

Fig. 7. The accelerator voltage oscillates at 0.9 MHz from the $\pi/2$ mode.

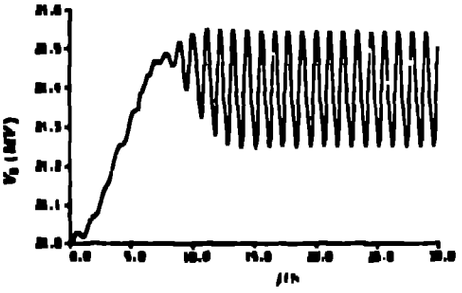

Fig. 8. The decelerator voltage oscillates with a half period displaced from the accelerator voltage

The threshold of inducing this instability in terms of the fraction of current lost is about 7.5%. For the system setup with total beam current of 46.2 mA, the threshold is about 5.0%.

By varying the beam-drift distance between the accelerator and the decelerator, the electron-arrival phase to the decelerator can be changed. When this is simulated, the voltage behavior at the accelerator and decelerator are identical, whether the beam is arriving earlier or later at the decelerator with the same magnitude of phase angle offset from the valley of the decelerating voltage.

Reference

1. T. F. Wang and H. Takeda, "RF Stability in the Los Alamos Free Electron Laser Energy Recovery Experiment," these proceedings.

2. D. W. Feldman, R. W. Warren, J. M. Watson, W. E. Stein, J. S. Fraser, G. Spalek, A. H. Lumpkin, B. E. Carlsten, H. Takeda, T. F. Wang, and C. A. Brau, "The Los Alamos Free Electron Laser Energy Recovery Experiment," these proceedings.